AIP | Applied Physics Letters

Anisotropic meta-mirror for achromatic electromagnetic polarization manipulation

Mingbo Pu, Po Chen, Yanqin Wang, Zeyu Zhao, Cheng Huang, Changtao Wang, Xiaoliang Ma, and Xiangang Luo

Citation: Applied Physics Letters **102**, 131906 (2013); doi: 10.1063/1.4799162
View online: http://dx.doi.org/10.1063/1.4799162
View Table of Contents: http://scitation.aip.org/content/aip/journal/apl/102/13?ver=pdfcov
Published by the AIP Publishing

Anisotropic meta-mirror for achromatic electromagnetic polarization manipulation

Mingbo Pu,[1] Po Chen,[2] Yanqin Wang,[1] Zeyu Zhao,[1] Cheng Huang,[1] Changtao Wang,[1] Xiaoliang Ma,[1] and Xiangang Luo[1,a)]
[1]*State Key Laboratory of Optical Technologies on Nano-Fabrication and Micro-Engineering, Institute of Optics and Electronics, Chinese Academy of Science, P.O. Box 350, Chengdu 610209, China*
[2]*Department of Geology and Geophysics, University of Wyoming, Laramie, Wyoming 82071, USA*

(Received 25 December 2012; accepted 19 March 2013; published online 3 April 2013)

Polarization states are of particular importance for the manipulation of electromagnetic waves. Here, we proposed the design and experimental demonstration of anisotropic meta-mirror for achromatic polarization tuning. It is demonstrated that linear polarized wave can be achromatically transformed to its cross-polarization state or to arbitrary circular polarization after its reflection from the mirror. Microwave experiments verified that the fraction bandwidth for 90% transformation efficiency can be larger than 3:1. Furthermore, by utilizing photoinduced carrier generation in silicon, a broadband tunable circular polarizer is demonstrated in the terahertz regime. © *2013 American Institute of Physics*. [http://dx.doi.org/10.1063/1.4799162]

Among all the properties of electromagnetic wave, polarization plays an important role since a majority of phenomena are polarization sensitive. Manipulation of polarization by material has been a hot topic for quite a long time.[1–15] It is well known that polarization states of light can be changed by natural occurring anisotropic media. As the two axes possess different refractive index (n_+ and n_-), a relative phase shift between the two axes $\Delta\Phi = \Phi_x - \Phi_y$ can be obtained. Without the loss of generality, $\Delta\Phi = \pi/2$, π, and $3\pi/2$ are required for the transformation of a linear polarized wave to the left handed circular polarization (LCP), cross polarization, and right handed circular polarization (RCP). However, as the difference between n_+ and n_- is typically very small, a large thickness is required to obtain a certain phase shift. Moreover, the working bandwidth is narrow because $\Delta\Phi$ is frequency dependent.

In the last decade, metamaterial has been widely utilized to realize polarization control based on its huge anisotropy[4,8] and (or) optical activity.[5,7] Many techniques were adopted to extend the working bandwidth. For instance, a three dimensional metallic helix array was used as a broadband circular polarizer in the infrared spectrum.[10] A biologically inspired achromatic wave-plate was realized for visible light.[16] Except from their huge anisotropy and (or) optical activity, metamaterial polarizers provide a simple approach for the dynamical tuning of polarization by embedding semiconductor parts between their metallic parts.[17–22] More recently, Zhang *et al.* reported the dynamic switching of optical activity and handedness of circular polarization by utilizing photoinduced carrier generation in silicon pads in the terahertz regime.[23]

Reflective meta-surface (we refer to such a device as "meta-mirror") is also proposed as an alternative way for the manipulation of polarization states.[4,12,14,24] In 2007, Zhou *et al.* proposed a circular polarizer based on an ultrathin metamaterial reflector.[4] Bozhevolnyi *et al.* also obtained similar phenomenon at optical frequencies using orthogonally oriented electrical dipoles.[12] Compared to the transmissive polarization transformer, meta-mirror has much smaller thickness due to the large anisotropy as well as higher energy efficiency since no complicate anti-reflection technique is applied. Furthermore, as a combination of mirror and polarization transformer, such meta-mirror can possess both the two functions in a single component, which is beneficial to the related systems such as terahertz and optical communications.[15]

In this letter, we take advantage of the huge anisotropy in artificial meta-mirror to decrease the thickness. Meanwhile, the frequency dispersion of the structure is exploited to achieve broadband achromatic performance. A technique for dynamic manipulation of polarization states is proposed in the terahertz regime. Both continuous tuning and discrete switching are demonstrated. As shown in Figs. 1(a) and 1(b), the meta-mirror proposed here is composed of an anisotropic metamaterial surface (meta-surface), a metallic reflective plane (for example, gold), and a dielectric spacer between them. Since we only consider the non-magnetic case, the reflective phase is mainly determined by the impedance along the direction where an electric field is applied. Thus, the phase difference between the two directions can be calculated separately. As illustrated in Fig. 1(c), the meta-mirror can be designed to realize arbitrary polarization transformations depending on the specific phase shift.

In general, the impedance sheet for both x and y directions can be both frequency dependent. We set Z_x as constant ($Z_x = \infty$) and Z_y as highly dispersive. Since the dielectric spacer is chosen as air ($n = 1$), the phase shift after the reflection can be calculated directly from the well-established transfer matrix method[25]

$$\begin{aligned}\Phi_x &= \pi + 2kd \\ \Phi_y &= \arg\left(\frac{-Z_0/Z_y - (2 - Z_0/Z_y)\exp(i2kd)}{2 + Z_0/Z_y - Z_0/Z_y\exp(i2kd)}\right),\end{aligned} \tag{1}$$

where k is the wave vector in free space and d is the thickness of dielectric spacer. The optimal impedance for a certain relative phase shift $\Delta\Phi$ can be calculated as

a)Author to whom correspondence should be addressed. Electronic mail: lxg@ioe.ac.cn.

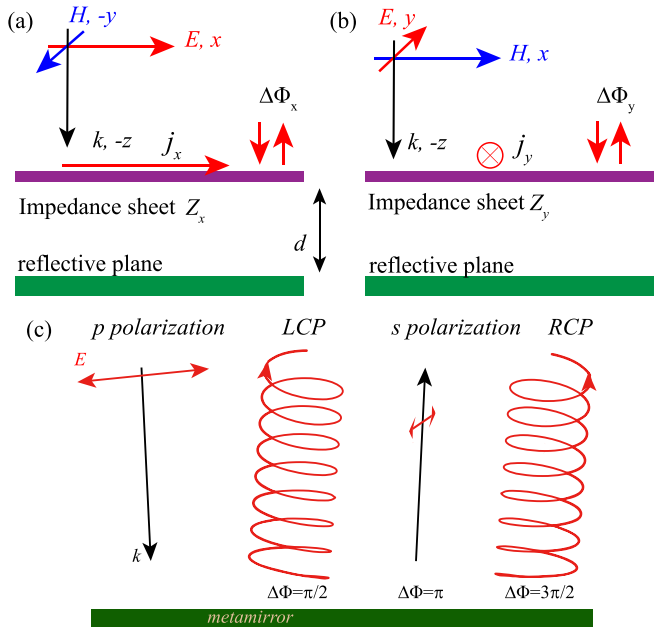

FIG. 1. Schematic of the anisotropic meta-mirror along (a) x and (b) y directions. (c) Schematic of polarization transformation for a p-polarization incident wave.

$$\frac{Z_y}{Z_0} = -\frac{1}{2}\frac{A - AB + 1 - B}{A + B}, \tag{2}$$

where $A = \exp(i(\Delta\Phi + 2kd + \pi))$ and $B = \exp(i2kd)$. Subsequently, the optimal impedances required for the perfect polarization control can be obtained. As shown in Fig. 2(a), the optimal impedances for $\Delta\Phi = \pi/2$, π, and $3\pi/2$ are calculated, which vary slightly with working frequency. In particular, the required impedance for $\Delta\Phi = \pi/2$ is mainly capacitive within the whole frequency range. For $\Delta\Phi = \pi$, however, the curve is separated to one capacitive region and the other inductive region at the two sides of the center frequency ($f = 0.25\, c/d$, where c is the speed of light). For $\Delta\Phi = 3\pi/2$, the requirement becomes mainly inductive within the entire frequency range.

Once the optimal impedance is obtained, the meta-surface can be used to realize it in a wide frequency band. As shown in Fig. 2(b), the unit cell of meta-surface used is composed of two metallic wires being connected with a pair of metallic patches. When the electric field is along y direction, the structure can be treated as a combination of an effective inductor L and capacitor C. The corresponding effective sheet impedance is $Z_y = j\omega L + 1/(j\omega C)$. From the electromagnetic field distribution, one can see that the inductance is contributed by the two thin wires and the capacitance stems from the parallel patch pairs. When the electric field is along x direction, the structure behaves as air since no inductive currents are induced.

In order to verify the above design principle, the geometric parameters (p_x, p_y, l, w, w_1, g, and t) are optimized to achieve $\Delta\Phi = \pi$ (design A) and $\Delta\Phi = 3\pi/2$ (design B). In the optimization, the length and width of the wires are used to tune the inductance while the length and separation of the patch pairs are utilized to adjust the capacitance. The effective sheet impedance of the metamaterial surface is retrieved using S parameters.[25,26]

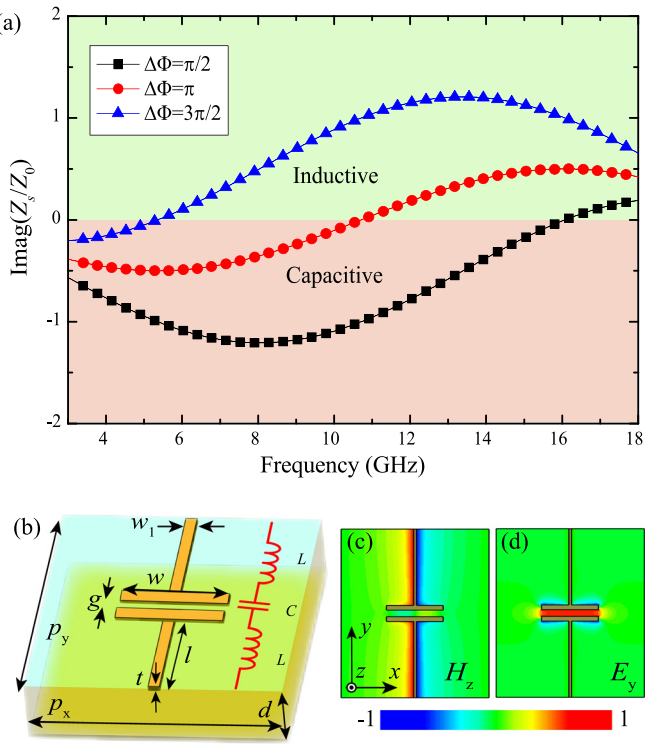

FIG. 2. (a) Imaginary parts of the optimal sheet impedances for $\Delta\Phi = \pi/2$, π, and $3\pi/2$. The real part is zero since no material loss is considered. The region above zero is inductive and the region below zero is capacitive. (b) Schematic of the unit cell of meta-mirror. (c) Magnetic field along z direction, which is related to the inductance L. (d) Electric field distribution along y axis, which determines the capacitance C. The values in (c) and (d) are normalized with their maxima.

In numerical simulation, finite element method (FEM) is utilized with periodic boundary condition along x and y directions. The metallic parts are made of copper of a conductivity of 5×10^7 S/m. The dielectric substrate is chosen as 0.5 mm thick with a permittivity of 2.5. For design A, the geometric parameters are optimized as $p_x = 5.2$ mm, $p_y = 7.4$ mm, $l = 3.35$ mm, $w = 2$ mm, $w_1 = 0.1$ mm, $g = 0.3$ mm, and $t = 0.035$ mm. For design B, $p_x = 11$ mm, $p_y = 16$ mm, $l = 7.35$ mm, $w = 3.6$ mm, $w_1 = 0.2$ mm, $g = 0.7$ mm, and $t = 0.035$ mm. As illustrated in Fig. 3(a), $\Delta\Phi_A$ is in the range of $(0.9\ \pi,\ 1.1\ \pi)$ for 5.1 GHz $<$ f $<$ 16.8 GHz. For $\Delta\Phi_B = (1.4\pi,\ 1.6\pi)$, the working frequency range becomes 4.1 GHz $<$ f $<$ 14.5 GHz. These properties can be further verified by the effective sheet impedance. As shown in Fig. 3(b), there are three intersection points between the optimal impedance and equivalent impedance. As a result, three frequency bands for near perfect polarization transformation as well as a broadband achromatic polarization transforming meta-mirror can be obtained.

Subsequently, the LC parameters for designs A and B are fitted as $L_1 = 3.67$ nH, $C_1 = 0.078$ pF, $L_2 = 8$ nH, and $C_2 = 0.13$ pF. Since L_2 is much larger than L_1, the period of unit cells becomes longer. In this case, the period is still smaller than the working wavelength at 18 GHz ($\lambda = 16.7$ mm). Thus, there is no grating lobe problem and the equivalent sheet impedance model is still valid. In fact, the meta-surface can be described by a lossless Lorentz model according to the equivalence of sheet impedance with permittivity[26]

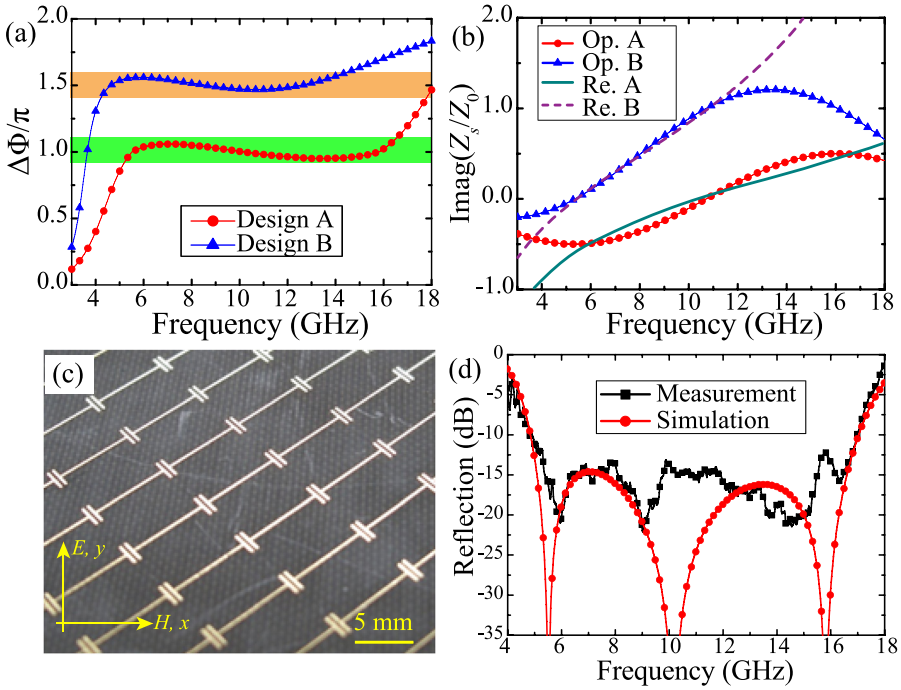

FIG. 3. (a) Relative phase differences for designs *A* and *B*. (b) Sheet impedances retrieved from *S* parameters (denoted as Re.A and Re.B) and the corresponding optimal impedance (denoted as Op.A and Op.B). (c) Photograph of the fabricated sample (design A). (d) Measured and simulated reflection coefficient for *x*-polarized incidence.

$$\varepsilon_{eff} = 1 + \frac{\omega_1^2}{\omega_0^2 - \omega^2}, \tag{3}$$

where $\omega_0 = (LC)^{-1/2}$ denotes the oscillation frequency of the bound electron in the meta-surface, while $\omega_1 = (\varepsilon_0 Lt)^{-1/2}$ is the density of electrons, which is related to the thickness t of the meta-surface.

In order to prove the above numerical results experimentally, a sample of design *A* with 40×40 unit cells is fabricated using PCB technology. In the measurement of *S* parameters, two standard linearly polarized (the electric field is parallel with *x* axis) horn antennas are connected to the two ports of a vector network analyzer R&S ZVA40. The sample is rotated 45° with respect to the *x* axis so that the *x*-polarized wave is transformed to *y*-polarization. In addition, the incident angle is set as 5°, which is a good approximation of the normal incidence. As shown in Fig. 3(d), the simulated reflection coefficient is below −15 dB in the frequency range between 5.5 and 16.5 GHz. The small difference between the measurement and simulation results is attributed to the cross-polarization of the two horn antennas.

It is interesting to note that the reflection coefficient is similar to a broadband absorber, where the incident wave is absorbed by material loss in the structure.[26] The difference between the two phenomena lies in the fact that the meta-mirror reflects the specifically linearly polarized incident wave to its orthogonal polarization while cannot be detected by the emitter with the same polarization. This is especially important for circular polarizations as they are insensitive to the azimuthal angle. For circular polarization, the reflection wave keeps its handedness, which is completely different from traditional mirror, where LCP is transformed into RCP after the reflection, and vice versa.

Although the principle of polarization transformation in meta-mirror is only demonstrated in microwave region, the structure proposed can be extended to higher frequencies such as terahertz and infrared frequencies due to the scalability of Maxwell's equations. Furthermore, as the structure is a combination of metallic and dielectric components, the structure can be designed as a tunable and achromatic polarization transformer by replacing some components with semiconductors.[18,23,24] It is well known that the optical and electrical performances of semiconductor such as silicon can be dynamically tuned through photoinduced carrier generation. When the photon energy is greater than the bandgap of silicon, the excited photocarriers transform the embedded silicon pads from insulator to good conductor.[18]

As illustrated in Fig. 4(a), two silicon pads are embedded between the metallic (gold) wires and patches in the unit cell of tunable meta-mirror. The silicon pads can introduce additional impedance dependent on the illuminated light intensity, which is essential for the dynamical tuning of polarization. The fabrication process of the structure is similar with that shown in the previous article.[23] After the preparation of silicon film, the silicon pads can be fabricated by photo-lithography and reactive ion etching. Then, the gold wires and patches are patterned by a second photo-lithography. In the simulation, the dielectric spacer is of a thickness of 95 μm and permittivity of 2.1. The gold wires are simulated as lossy metal with a conductivity of 7×10^6 S/m. The permittivity of silicon is set as 11.7 while the maximal conductivity under the optical illumination is chosen to be 50 000 S/m, corresponding to a carrier density of 2.5×10^{18} cm^3 and photoexcitation power of 500 mW.[19]

There are two design goals which should be satisfied in the optimization: the first is $\Delta\Phi = \mathrm{A}$ for the case without optical illumination and the other is $\Delta\Phi = \mathrm{B}$ under strong optical illumination. As an example, the condition $\mathrm{A} = 0$ and $\mathrm{B} = 3\pi/2$ are used, corresponding to a switchable circular polarizer. The geometrical parameters are optimized using FEM method at near normal incidence as $p_x = 300\ \mu$m, $p_y = 150\ \mu$m, $l = 35\ \mu$m, $w = 70\ \mu$m, $w_1 = 7\ \mu$m, $g = 13\ \mu$m, and $t = 0.5\ \mu$m. The dimensions of the silicon pads are $30\ \mu\text{m} \times 25\ \mu\text{m} \times 1\ \mu$m. The phase shifts $\Delta\Phi$ for the

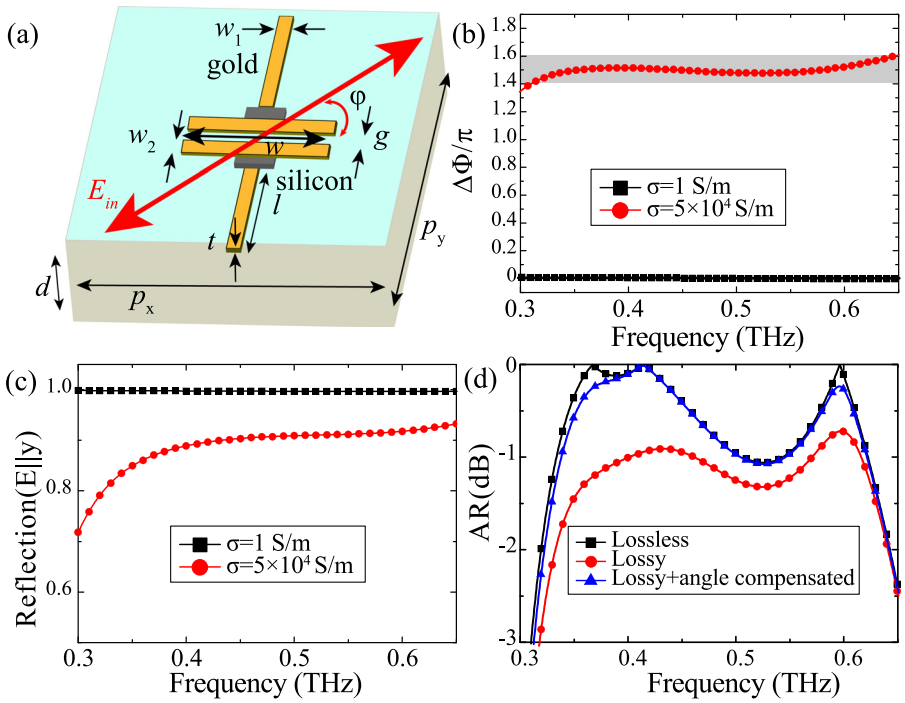

FIG. 4. (a) Schematic of the unit cell of the tunable terahertz meta-mirror. (b) Calculated relative phase differences for different conductivities. (c) Amplitudes of reflection coefficients of for *y*-polarized wave. (d) Axial ratios of the reflected circular polarized wave for the lossy, lossless, and angle compensated cases. In the angle compensation case, the azimuthal angle is 48.15°.

insulating and conducting cases are illustrated in Fig. 4(b). At the absence of optical illumination, the phase shift is zero as if the meta-surface is isotropic. Under strong optical excitation, the silicon behaves like metal and the polarization can be transformed after the reflection. The corresponding phase shift in frequencies between 0.32 and 0.65 THz is within $(1.4\pi, 1.6\pi)$.

As shown in Fig. 4(c), the reflection amplitude of *y*-polarized components under optical illumination is smaller than unit, which is resulted from the absorption in silicon (the maximum conductivity of silicon is much smaller than noble metal). The influence of absorption can be weakened by an angle compensation technique. As shown in Fig. 4(a), the polarization angle of electric field is φ with respect to x axis. If one choose $r_x \cos\varphi = r_y \sin\varphi$, the reflection wave is still in circular polarization. Here, r_x and r_y are the average reflection coefficients for *x*- and *y*-polarized waves. As depicted in Fig. 4(d), the axial ratios (*AR*s) of the circular polarization are calculated by $AR = -20\log(\max(E)/\min(E))$ for the cases of no absorption, absorption, and angle compensation, where $\max(E)$ and $\min(E)$ are corresponding to the long and short axes of the polarization eclipses. Clearly, the *AR* of angle compensated reflection is close to the case without loss.

In summary, we proposed the theoretical design, numerical simulation, and experimental demonstration of meta-mirror with the capability of broadband achromatic polarization manipulation. The frequency dispersion of the meta-mirror is optimized to compensate the phase shift induced by frequency change. Furthermore, the optical induced photo-carrier generation effect in silicon is utilized to dynamically tune the broadband polarizer. The achromatic meta-mirror proposed is useful in a variety of applications ranging from stealth technology to terahertz communications.

This work was supported by 973 Program of China (No. 2011CB301800) and National Natural Science Funds (No. 61138002).

[1]Lord Rayleigh, Philos. Mag. **41**, 107 (1871).
[2]G. Nordin and P. Deguzman, Opt. Express **5**, 163 (1999).
[3]J.-B. Masson and G. Gallot, Opt. Lett. **31**, 265 (2006).
[4]J. Hao, Y. Yuan, L. Ran, T. Jiang, J. A. Kong, C. T. Chan, and L. Zhou, Phys. Rev. Lett. **99**, 063908 (2007).
[5]B. Bai, Y. Svirko, J. Turunen, and T. Vallius, Phys. Rev. A **76**, 023811 (2007).
[6]J. Y. Chin, M. Lu, and T. J. Cui, Appl. Phys. Lett. **93**, 251903 (2008).
[7]E. Plum, V. A. Fedotov, and N. I. Zheludev, Appl. Phys. Lett. **93**, 191911 (2008).
[8]J. Zhao, Y. Chen, and Y. Feng, Appl. Phys. Lett. **92**, 071114 (2008).
[9]M. Decker, M. Ruther, C. E. Kriegler, J. Zhou, C. M. Soukoulis, S. Linden, and M. Wegener, Opt. Lett. **34**, 2501 (2009).
[10]J. K. Gansel, M. Thiel, M. S. Rill, M. Decker, K. Bade, V. Saile, G. von Freymann, S. Linden, and M. Wegener, Science **325**, 1513 (2009).
[11]X. G. Peralta, E. I. Smirnova, A. K. Azad, H.-T. Chen, A. J. Taylor, I. Brener, and J. F. O'Hara, Opt. Express **17**, 773 (2009).
[12]A. Pors, M. G. Nielsen, G. D. Valle, M. Willatzen, O. Albrektsen, and S. I. Bozhevolnyi, Opt. Lett. **36**, 1626 (2011).
[13]X. Ma, C. Huang, M. Pu, C. Hu, Q. Feng, and X. Luo, Opt. Express **20**, 16050 (2012).
[14]E. Doumanis, G. Goussetis, J. L. Gómez-Tornero, R. Cahill, and V. Fusco, IEEE Trans. Antennas Propag. **60**, 212 (2012).
[15]D. L. Markovich, A. Andryieuski, M. Zalkovskij, R. Malureanu, and A. V. Lavrinenko, "Metamaterial polarization converter analysis: limits of performance," Appl. Phys. B (2013).
[16]Y.-J. Jen, A. Lakhtakia, C.-W. Yu, C.-F. Lin, M.-J. Lin, S.-H. Wang, and J.-R. Lai, Nat. Commun. **2**, 363 (2011).
[17]O. Reynet and O. Acher, Appl. Phys. Lett. **84**, 1198 (2004).
[18]H.-T. Chen, W. J. Padilla, J. M. O. Zide, A. C. Gossard, A. J. Taylor, and R. D. Averitt, Nature **444**, 597 (2006).
[19]H.-T. Chen, J. F. O'Hara, A. K. Azad, A. J. Taylor, R. D. Averitt, D. B. Shrekenhamer, and W. J. Padilla, Nat. Photonics **2**, 295 (2008).
[20]H.-T. Chen, S. Palit, T. Tyler, C. M. Bingham, J. M. O. Zide, J. F. O'Hara, D. R. Smith, A. C. Gossard, R. D. Averitt, W. J. Padilla, N. M. Jokerst, and A. J. Taylor, Appl. Phys. Lett. **93**, 091117 (2008).
[21]G. V. Naik and A. Boltasseva, Phys. Status Solidi (RRL) **4**, 295 (2010).
[22]J. Gu, R. Singh, X. Liu, X. Zhang, Y. Ma, S. Zhang, S. A. Maier, Z. Tian, A. K. Azad, H.-T. Chen, A. J. Taylor, J. Han, and W. Zhang, Nat. Commun **3**, 1151 (2012).
[23]S. Zhang, J. Zhou, Y.-S. Park, J. Rho, R. Singh, S. Nam, A. K. Azad, H.-T. Chen, X. Yin, A. J. Taylor, and X. Zhang, Nat. Commun. **3**, 942 (2012).
[24]B. Zhu, Y. Feng, J. Zhao, C. Huang, Z. Wang, and T. Jiang, Opt. Express **18**, 23196 (2010).
[25]M. Pu, C. Hu, M. Wang, C. Huang, Z. Zhao, C. Wang, Q. Feng, and X. Luo, Opt. Express **19**, 17413 (2011).
[26]Q. Feng, M. Pu, C. Hu, and X. Luo, Opt. Lett. **37**, 2133 (2012).